

Supplementary Information

Amorphous and crystalline calcium carbonate phases during carbonation of nanolimes: Implications in heritage conservation

Carlos Rodriguez-Navarro,^{a*} Kerstin Elert,^a and Radek Ševčík^b

^a Dpto. Mineralogía y Petrología, Universidad de Granada, Fuentenueva s/n, 18071 Granada, Spain

^b Institute of Theoretical and Applied Mechanics AS CR, Centre of Excellence Telč, Batelovská 485-486, 588 56 Telč., Czech Republic

*Correspondence to: carlosrn@ugr.es

Table of contents	Page
Fig. S1. Nanolime characterization.	S2
Fig. S2. FESEM images of portlandite nanoparticles subjected to 3 h carbonation in air at room <i>T</i> .	S3
Fig. S3. XRD patterns of <i>t</i> -dependent CaCO ₃ phase evolution during nanolime carbonation.	S4
Fig. S4. FESEM images of calcite crystals in partially carbonated nanolime. After 24 h carbonation time.	S5
Fig. S5. In situ Raman spectroscopy analysis of nanolime carbonation following oven-drying of the nanolime dispersion (1 h at 100°C).	S6
Fig. S6. XRD patterns of nanolime subjected to oven-drying (1 h at 100°C) and carbonation in air at 80 % RH.	S7
Supplementary references	S8

Supplementary Figures

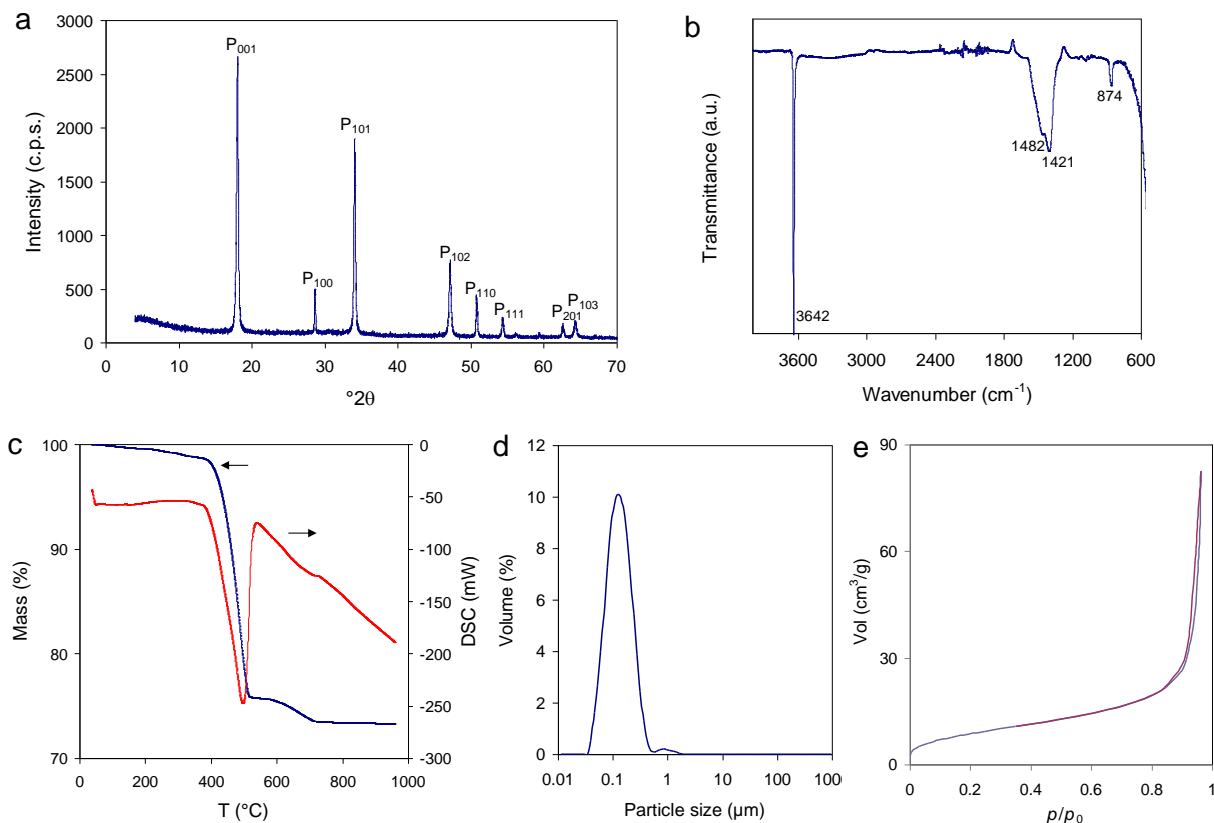


Fig. S1. Nanolime characterization. XRD (a), FTIR (b), and TG/DSC (c) analyses show that the nanolime was made up of portlandite ($\text{Ca}(\text{OH})_2$) crystals with minor amounts of CaCO_3 (≤ 5.2 wt%). The presence of CaCO_3 was likely due to the unavoidable partial carbonation taking place during oven drying of the alcohol dispersion (to obtain powder samples) prior to analysis. However, the XRD pattern (a) showed no Bragg peaks corresponding to any crystalline CaCO_3 polymorph. The FTIR spectrum (b) showed, in addition to the intense and sharp O-H stretching band at 3642 cm^{-1} corresponding to crystalline $\text{Ca}(\text{OH})_2$, a weak broad band centered at 3450 cm^{-1} corresponding to the O-H stretching in H_2O , plus a broad band at $1482\text{--}1421\text{ cm}^{-1}$ and a band at 867 cm^{-1} corresponding to the ν_3 and ν_2 modes of carbonate groups, respectively. However, no bands at 713 , 745 , or $712\text{--}700\text{ cm}^{-1}$ corresponding to crystalline calcite, vaterite or aragonite, respectively, were detected. In addition, the TG trace (c) showed a limited weight loss at $100\text{--}350\text{ }^\circ\text{C}$ which does not correspond to the dehydroxylation of portlandite (it takes place at $350\text{--}550\text{ }^\circ\text{C}$), but to the dehydration of ACC.^{S1} All together, these results show that the carbonate phase present in minor amounts was ACC.^{S2} The average size of the nanoparticles determined by laser scattering was $34\text{--}400\text{ nm}$ (mode = 138 nm) (d). The N_2 sorption isotherm (e) revealed that the $\text{Ca}(\text{OH})_2$ nanoparticles displayed a type II isotherm, with H_3 hysteresis loop, typical of plate-like mesoporous solids with slit-shaped interparticle pores. These features are typical of $\text{Ca}(\text{OH})_2$ particles prepared either via homogeneous or heterogeneous synthesis (i.e., slaked lime).^{S3-S5}

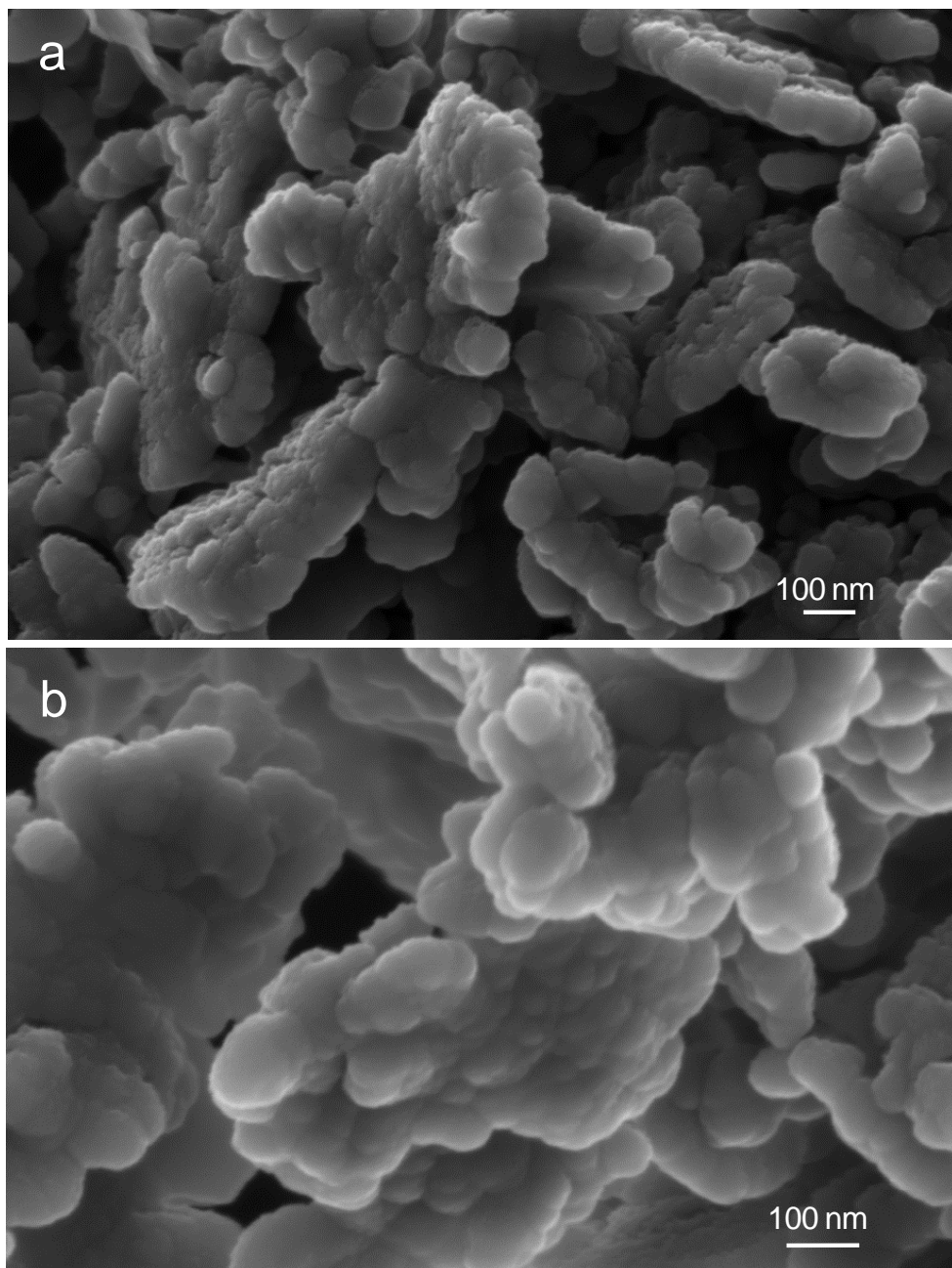


Fig. S2. FESEM images of portlandite nanoparticles subjected to 3 h carbonation in air at room T . a) General overview of the porous structure undergoing carbonation. Each individual $\text{Ca}(\text{OH})_2$ nanoparticle is being transformed and covered by ACC nanoparticles; b) Detail of nanogranular ACC covering individual portlandite nanoparticles. Note that at this stage, XRD analysis does not show the presence of any crystalline CaCO_3 .

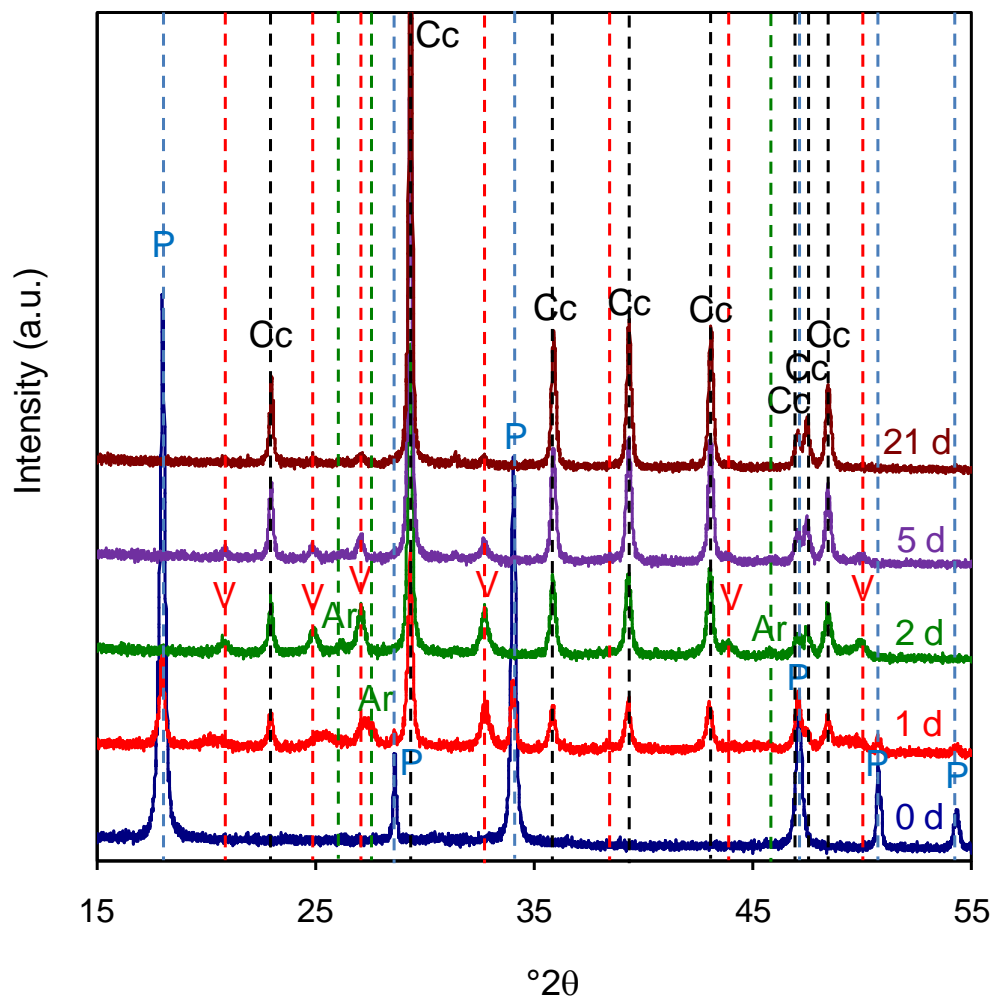


Fig. S3. XRD patterns of t -dependent CaCO_3 phase evolution during nanolime carbonation.
 Legend: P, portlandite; Cc, calcite; V, vaterite; Ar, aragonite.

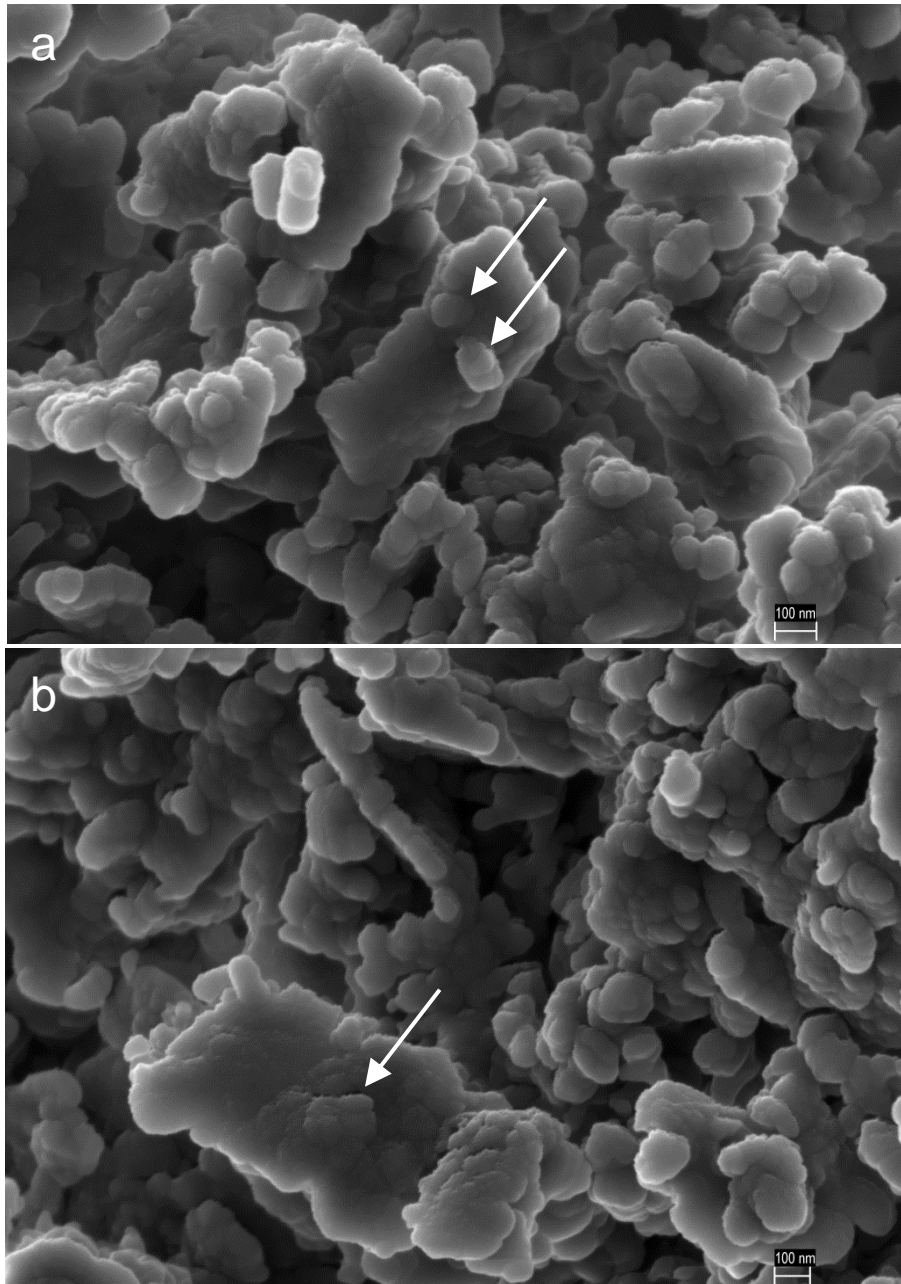


Fig. S4. FESEM images of calcite crystals in partially carbonated nanolime. After 24 h carbonation time, nanogranules, presumably ACC nanoparticles (arrows), are observed on calcite rhombohedra both in (a) and (b).

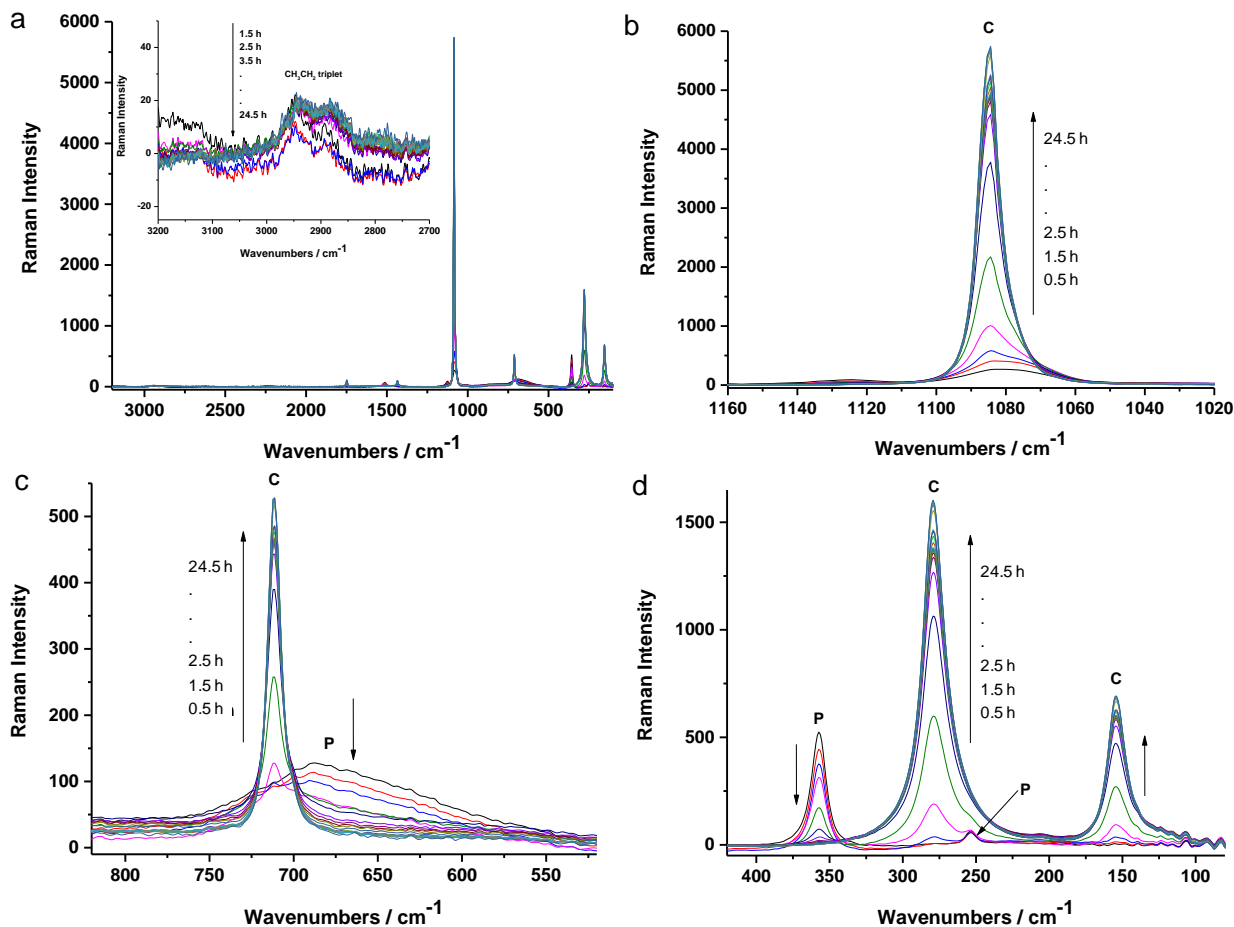


Fig. S5. In situ Raman spectroscopy analysis of nanolime carbonation following oven-drying of the nanolime dispersion (1 h at 100°C). a) Raman spectra corresponding to all analyses collected over the 24.5 h carbonation time. The inset shows a detail of the spectral region corresponding to alcohol (i.e., C-H stretching mode of CH₂ and CH₃ groups in ethanol). Note that the Raman intensity of these bands is negligible. Details of relevant spectral regions showing the formation of different calcium carbonate phases (b, c, and d). Note that during the early stages of carbonation the band at ~1080 cm⁻¹ (b) shows a shoulder that corresponds to ACC. This band shifts to higher wavenumbers as carbonation progresses and calcite becomes the dominant phase. Legend: P, portlandite, C, calcite.

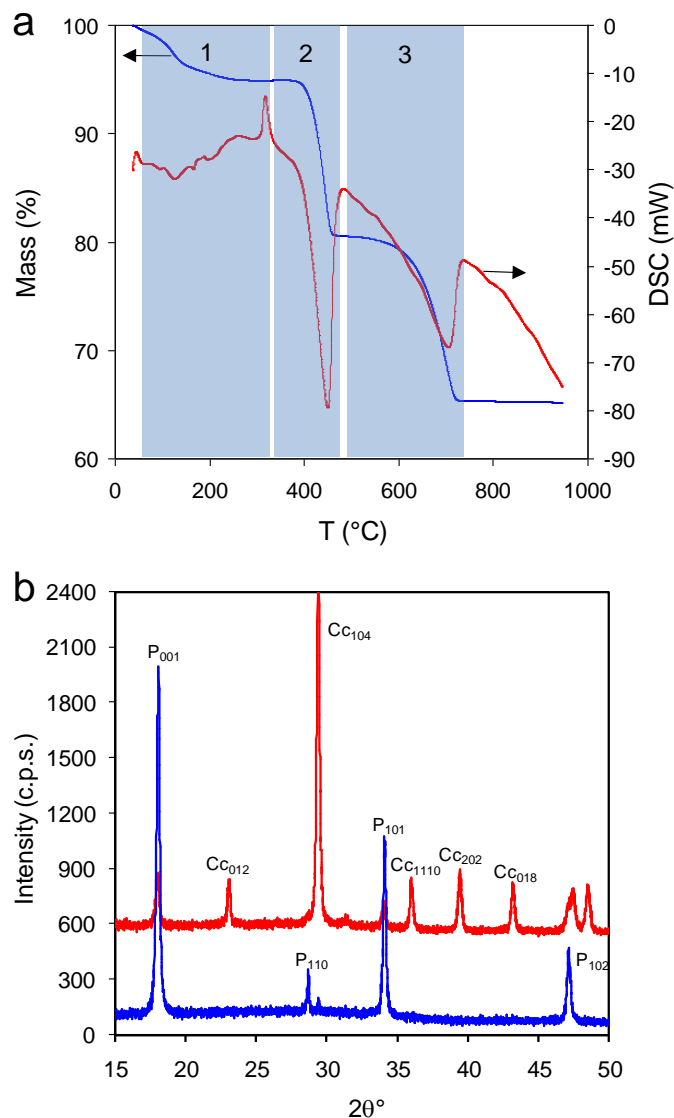


Fig. S6. TG/DSC and XRD analyses of nanolime subjected to oven-drying (1 h at 100 °C) followed by carbonation for 6 h in air (80 %RH) at room T . a) TG/DSC traces show a marked weight loss at 100-350 °C (shaded area 1) and an exothermal peak at 320 °C, corresponding to the dehydration and crystallization of ACC (~27 wt%).^{S1} Shaded areas (2) and (3) correspond to dehydroxylation of portlandite and decomposition of calcite, respectively; b) the XRD pattern of the sample subjected to 6 h carbonation shows no Bragg peaks of crystalline CaCO_3 , other than a minor 104_{calcite} peak corresponding to trace amounts of this phase (blue pattern). In contrast, heating this sample to 350 °C for 1 h, results in intense calcite Bragg peaks (red pattern). These results show that carbonation of nanolime subjected to (almost complete) ethanol desorption (after 1 h heat treatment at 100 °C) involves the formation of ACC during the early stages of carbonation. Subsequently, ACC transforms into calcite (in agreement with Raman analysis; Fig. S8). The significant reduction in the intensity of portlandite Bragg peaks after heating at 350 °C is likely due to the transformation of ACC into calcite, a denser phase, forming a surface shield that reduced the intensity of x-rays diffracted by the underlying portlandite crystals. Legend: P, portlandite, Cc, calcite.

Supplementary references

- S1) N. Koga and Y. Yamane, *J. Therm. Anal. Calorimetry*, 2008, **94**, 379-387.
- S2) L. Addadi, S. Raz and S. Weiner, *Adv. Mater.*, 2003, **15**, 959-970.
- S3) D. T. Beruto and R. Botter, *J. Eur. Ceram. Soc.*, 2000, **20**, 497-503.
- S4) C. Rodriguez-Navarro, E. Ruiz-Agudo, M. Ortega-Huertas and E. Hansen, *Langmuir*, 2005, **21**, 10948-10957.
- S5) C. Rodriguez-Navarro, A. Suzuki and E. Ruiz-Agudo, *Langmuir*, 2013, **29**, 11457-11470.